



OPEN

SRT1720 improves survival and healthspan of obese mice

SUBJECT AREAS:

METABOLISM

ANIMALS

PHARMACOLOGY

DISEASES

Received
18 July 2011Accepted
29 July 2011Published
18 August 2011Correspondence and
requests for materials
should be addressed to
R.deC. (decabora@
mail.nih.gov)

Robin K. Minor¹, Joseph A. Baur², Ana P. Gomes³, Theresa M. Ward¹, Anna Csiszar⁴, Evi M. Mercken¹, Kotb Abdelmohsen⁵, Yu-Kyong Shin⁶, Carles Canto⁷, Morten Scheibye-Knudsen⁸, Melissa Krawczyk⁹, Pablo M. Irueta^{1,10}, Alejandro Martín-Montalvo¹, Basil P. Hubbard³, Yongqing Zhang¹¹, Elin Lehrmann¹¹, Alexa A. White⁶, Nathan L. Price³, William R. Swindell¹², Kevin J. Pearson^{1,13}, Kevin G. Becker¹¹, Vilhelm A. Bohr⁸, Myriam Gorospe⁵, Josephine M. Egan⁶, Mark I. Talan⁹, Johan Auwerx⁷, Christoph H. Westphal¹⁴, James L. Ellis¹⁴, Zoltan Ungvari⁴, George P. Vlasuk¹⁴, Peter J. Elliott¹⁴, David A. Sinclair³ & Rafael de Cabo¹

¹Laboratory of Experimental Gerontology, National Institute on Aging, National Institutes of Health, 251 Bayview Boulevard, Baltimore, MD 21224, USA, ²Department of Physiology, Institute for Diabetes, Obesity, and Metabolism, University of Pennsylvania School of Medicine, 415 Curie Blvd, CRB 728, Philadelphia, PA 19104, USA, ³Paul F. Glenn Laboratories for the Biological Mechanism of Aging, Department of Pathology, Harvard Medical School, Boston, MA 02115, USA, ⁴Reynolds Oklahoma Center on Aging, Department of Geriatric Medicine, University of Oklahoma Health Sciences Center, 975 NE 10th Street, BRC-1303, Oklahoma City, OK 73104, USA, ⁵Laboratory of Cellular and Molecular Biology, National Institute on Aging, National Institutes of Health, 251 Bayview Boulevard, Baltimore, MD 21224, USA, ⁶Laboratory of Clinical Investigation, National Institute on Aging, National Institutes of Health, 251 Bayview Boulevard, Baltimore, MD 21224, USA, ⁷Laboratory of Integrative and Systems Physiology (IUSP), Ecole Polytechnique Fédérale de Lausanne (EPFL), CH-1015, Lausanne, Switzerland, ⁸Laboratory of Molecular Gerontology, National Institute on Aging, National Institutes of Health, 251 Bayview Boulevard, Baltimore, MD 21224, USA, ⁹Laboratory of Cardiovascular Sciences, National Institute on Aging, National Institutes of Health, 5600 Nathan Shock Drive, Baltimore, MD 21224, USA, ¹⁰Department of Human Science, Georgetown University Medical Center, Washington, DC, USA, ¹¹Gene Expression and Genomics Unit, National Institute on Aging, National Institutes of Health, 251 Bayview Boulevard, Baltimore, MD 21224, USA, ¹²Department of Genetics, Harvard Medical School, Boston, MA 02115, USA, ¹³Graduate Center for Nutritional Sciences, University of Kentucky, 900 South Limestone, C.T. Wethington Bldg, Rm 591, Lexington, KY 40536, USA, ¹⁴Sirtis, a GSK Company, 200 Technology Square, Cambridge, MA 02139, USA.

Sirt1 is an NAD⁺-dependent deacetylase that extends lifespan in lower organisms and improves metabolism and delays the onset of age-related diseases in mammals. Here we show that SRT1720, a synthetic compound that was identified for its ability to activate Sirt1 *in vitro*, extends both mean and maximum lifespan of adult mice fed a high-fat diet. This lifespan extension is accompanied by health benefits including reduced liver steatosis, increased insulin sensitivity, enhanced locomotor activity and normalization of gene expression profiles and markers of inflammation and apoptosis, all in the absence of any observable toxicity. Using a conditional SIRT1 knockout mouse and specific gene knockdowns we show SRT1720 affects mitochondrial respiration in a Sirt1- and PGC-1 α -dependent manner. These findings indicate that SRT1720 has long-term benefits and demonstrate for the first time the feasibility of designing novel molecules that are safe and effective in promoting longevity and preventing multiple age-related diseases in mammals.

As rates for obesity among humans continue to climb, both in the United States and worldwide, the global burden of obesity-related health consequences on quality and length of life—and healthcare spending—rises in lockstep. There is growing evidence that increased adiposity accelerates the aging process, primarily by promoting inflammation^{1,2} but also by suppressing the expression of longevity genes^{3,4}. One longevity gene that is suppressed by excess calorie intake is Sirt1, the mammalian ortholog of the NAD⁺-dependent deacetylase discovered by virtue of its ability to increase lifespan in lower organisms^{3,4}. Activation of Sirt1 with compounds such as resveratrol is believed to hold promise as a countermeasure for diseases accelerated by obesity and aging in mammals^{5,6}. Indeed, in a previous study we found treatment of mice with resveratrol resulted in benefits to lifespan and healthspan (e.g. metabolic dysfunction and hepatic steatosis) in mice on a high-fat diet⁷, consistent with later reports that mice with additional Sirt1 also show improvements in measures of healthspan^{8,9}. However, given that resveratrol has a number of *in vivo* targets¹⁰, the extent to which its effects are mediated by Sirt1 is the subject of considerable debate.



SRT1720, a compound that activates Sirt1 *in vitro*¹¹, is one of a series of pharmaceutical compounds that are being investigated for their efficacy in the treatment of metabolic and chronic diseases associated with aging. In short-term *in vivo* studies, SRT1720 has been demonstrated to enhance insulin sensitivity and improve measures of mitochondrial capacity and oxidative metabolism in obese rats and mice^{11–13}. However, the long-term effects of SRT1720, as well as its ability to postpone diseases of aging, are currently unknown. Moreover a recent report has raised questions about the mechanism of action, metabolic effects and toxicity of SRT1720¹⁴. Both a recent *in vitro* study¹⁵ and this *in vivo* study comprehensively address these issues by providing further data that SRT1720 benefits multiple metabolic parameters, that Sirt1 is required for several of these effects, and that the compound is well tolerated in mice even when consumed daily in the diet over the greater part of the lifespan. Indeed, SRT1720 treatment of mice fed a high-fat diet increased lifespan in a dose-dependent manner. With regards to healthspan SRT1720 promoted a gene expression profile similar to mice on a lean diet while producing benefits to metabolism and organ structure and function.

Results

SRT1720 extends lifespan and confers hepatic and pancreatic protection in obese mice. To test the chronic effects of SRT1720 treatment we placed one-year old male C57BL/6J mice on a high-fat diet (HFD) with two doses of SRT1720 and monitored them for the remainder of their lifespan. As shown in Figure 1a, both mean and maximum lifespan were extended by SRT1720 treatment (data on dates of death for every mouse are included in Supplementary Table 1). Survival among the high fat groups was significantly different by the log-rank test ($\chi^2 = 70.4$, $P < 0.0001$), with mice fed a higher dose of SRT1720 (HFD-H; 100 mg/kg body weight) living longer than their HFD counterparts. From birth, mean lifespan extension from HFD in mice fed a lower dose of SRT1720 (HFD-L; 30 mg/kg) was 4% and HFD-H was 18%. From 56 weeks of age (the age at which interventions were begun), mean lifespan was increased 11% in HFD-L and 44% in HFD-H. Median lifespan was 125 weeks for SD, 94 weeks for HFD, 103 weeks for HFD-L and 115 for HFD-H. Maximum lifespan (computed from the longest-lived 10% per group) was significantly extended in the HFD-H group ($P = 0.01$) and the hazard ratio for death was significantly reduced ($\chi^2 = 20.0$, $P < 0.0001$, PHREG analysis of maximum likelihood estimates). Extension of maximum lifespan from HFD was 3% and 5% from birth and 6% and 9% from diet onset in the HFD-L and HFD-H groups, respectively. Likewise, the high dose of SRT1720 altered the hazard rate for mortality, shifting the curves towards those of the SD and away from the HFD (Supplementary Fig. 1).

Lifespan extension by SRT1720 occurred despite rapid and robust weight gain by all HFD groups compared with SD controls, as is apparent in the body weight curves over the course of the feeding study (Fig. 1b). Importantly, while all HFD groups consumed significantly more calories than the SD controls, there was no difference among the HFD groups in calorie consumption (Fig. 1b and Supplementary Fig. 1c). We also monitored SRT1720 levels in plasma at 120 weeks of age and, as expected, SRT1720 was undetectable in plasma from SD controls and was found in the highest concentration in plasma from the HFD-H mice (Supplementary Table 2).

Lifespan extension in the SRT1720-treated mice was accompanied by a profound reversal of the structural and functional deficits induced by the high fat diet in liver (Fig. 1c) and pancreas (Fig. 1d). In the liver (Fig. 1c) we observed a reduction in fat accumulation associated with consumption of a high-fat diet at 82 weeks of age, which was apparent even to the naked eye (note enlargement and pallid color of HFD liver inset compared with SD and HFD-H). Histological examination of liver sections stained with oil red O showed that

accumulation of lipid droplets in the livers of the HFD was more pronounced than in the SD or HFD-H group, and blinded scoring of the liver sections for steatosis on a scale of 0–4 (with 4 being the most severe) confirmed that the HFD-H livers were significantly less fatty than the HFD livers. These results corroborate data from a several mouse models of obesity, all of which showed reduced hepatic fat accumulation after SRT1720 treatment^{12,16,17}. Giving further support to the involvement of Sirt1 in reduced steatosis, these results are consistent with data from mice engineered with hepatocyte-specific overexpression of Sirt1¹⁸. Assessments of liver function via serum levels of the transaminases alanine aminotransferase (ALT) and aspartate aminotransferase (AST), which are released into circulation following hepatocellular damage, both indicate liver function is compromised in HFD mice. Treatment with the high dose of SRT1720 reduced both ALT and AST levels and the effect was greater for AST which was normalized to SD levels by SRT1720.

Many patients with type 2 diabetes will eventually need insulin due to the failure of pancreatic beta cells. Hence there is considerable interest in finding agents that preserve beta cell function. Activators of Sirt1 have not yet been examined in this regard. Staining of pancreata from the mice revealed islet area was increased in mice on the HFD but not in the HFD-H mice (Fig. 1d), indicating that SRT1720 protects against islet hypertrophy, a hallmark of the insulin resistance associated with obesity. Within islets, the percentage of islet area represented by α cells was reduced in both the HFD and HFD-H, although the reduction in the HFD-H was less than that in the HFD. It is interesting to note that secretion of glucagon during fasting is necessary to prevent neuroglycopenia, and, while this has not been reported, our results suggest that animals fed a high-fat diet have a reduced requirement for glucagon reflective of chronic caloric abundance. Regarding insulin production, the fraction of β cells present in the islets increased in the HFD, a common consequence of weight gain and associated insulin resistance. However, despite similar weight gain in the HFD-H animals, β cell area was significantly less than in the HFD.

SRT1720 improves body composition, glucose homeostasis and metabolism in mice on a high-fat diet. Gross changes to whole organ weight were noted among the diet groups (Fig. 2a) and, as anticipated, the reduced accumulation of fat in the livers of the HFD-H mice correlated with a reduction in liver mass compared with HFD mice assessed at 82 weeks of age. Livers from the HFD-L mice were also smaller than HFD livers, although both HFD-L and HFD-H livers were still somewhat larger than SD livers.

Heart and kidney mass, however, were not increased at all in the mice treated with SRT1720, only in untreated HFD mice. Assessments of other major pathological changes to organs at 82 weeks of age including heart, kidney, liver, spleen and lung are included in Supplementary Table 3a, and did not reveal major differences among the groups. No indication of toxicity by SRT1720 was noted in the mice at sacrifice or in necropsies performed after death in the remainder of the mice. Results from necropsies performed following spontaneous death revealed 6% of mice in the HFD group showed clear visual signs of ischemic foci in the heart (seen as pale areas of the tissue) while only 1% of hearts from the SD and HFD-L groups and none of the HFD-H indicated ischemia (Supplementary Table 3b). Further investigation of cardiac function by echocardiography revealed no significant differences among the treatment groups at 118 weeks of age in either heart rate or ejection fraction (Supplementary Fig. 3a,b). Presence of perirenal fat was only observed in the HFD groups and was highest in the untreated HFD group at 5% (Supplementary Table 3b). Visible hepatic steatosis at necropsy was greatest in the HFD group (43%) and was reduced by the low dose of SRT1720 (24%) and further by the high dose (11%), although the lowest incidence was in the SD group (4%) in agreement with the blinded pathological scoring results (Fig. 1c). These results are

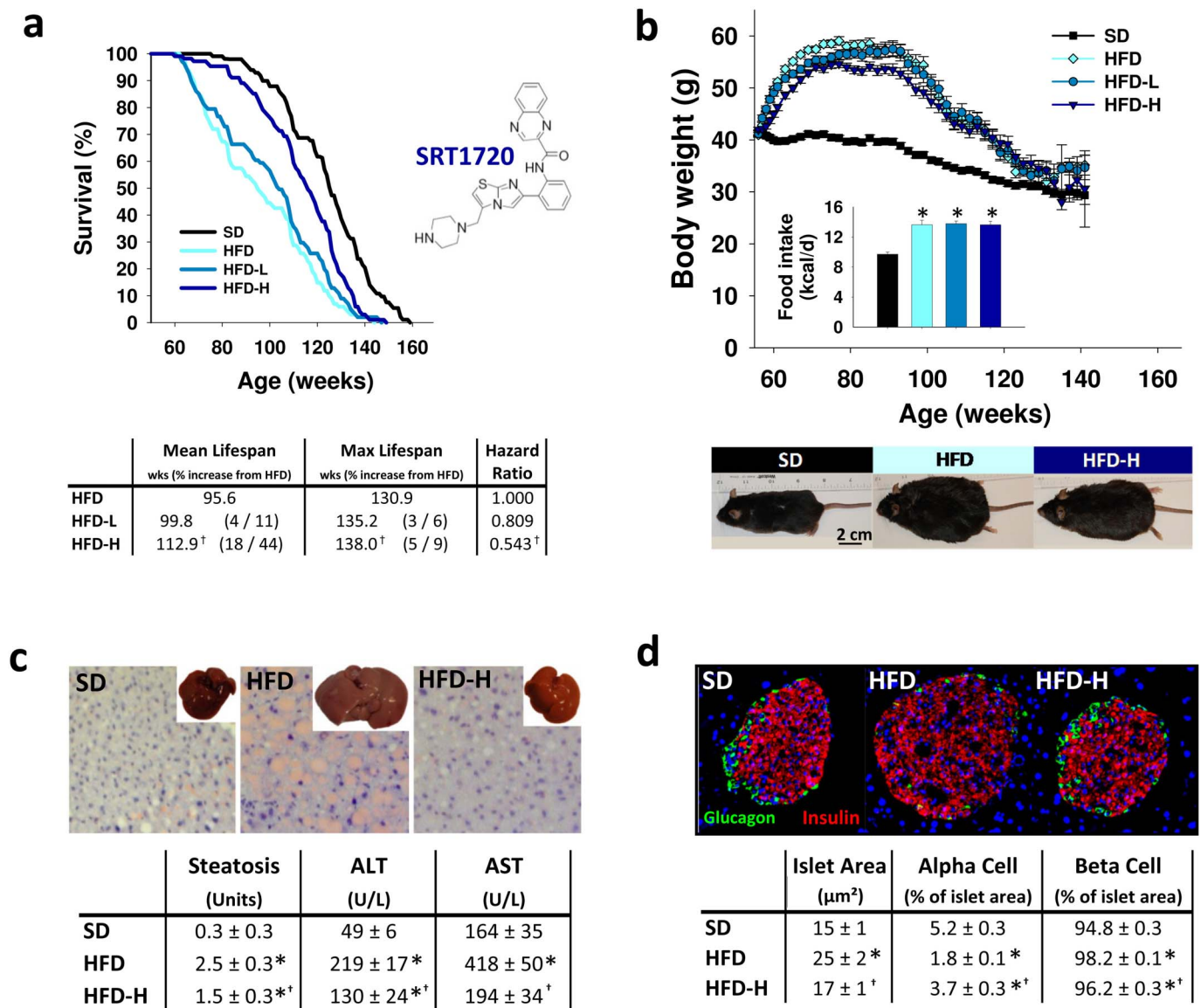


Figure 1 | SRT1720 extends lifespan and reverses organ pathology associated with a high-fat diet. (a) Kaplan-Meier survival curves of mice fed a standard diet (SD) or a high-fat diet (HFD) supplemented with SRT1720 at either a low (HFD-L) or high (HFD-H) dose. Mean and maximum lifespan in weeks and the hazard ratio for mortality are represented below. In the parentheses the increases in maximum lifespan from birth and then diet onset are given. (b) Body weights of the groups over time, with average caloric intake over the course of the feeding study in the inset. Below are images of representative mice to illustrate phenotypic body mass of the groups at 82 weeks of age. (c) SRT1720 maintained normal liver appearance and reduced the onset of fatty liver as depicted by images of whole livers harvested after 12 weeks on diets and subsequent oil red O staining. Quantification of steatosis was performed by a blinded pathologist on livers from 82 week-old mice (26 weeks on diets; $n = 6$). Serum levels of the aminotransferases ALT and AST were reduced by SRT1720 compared with HFD ($n = 6$; age = 82 wks; diet = 26 wks). (d) SRT1720 normalized pancreas morphology as illustrated by immunostaining for glucagon-producing cells (α cells, green) and insulin-producing cells (β cells, red) in islets, and quantification of islet area and relative α -cell and β -cell areas within the islets ($n = 8$; diet = 12 weeks). Data are represented as the mean \pm SEM. * $P < 0.0083$ from SD; [†] $P < 0.0083$ from HFD.

consistent with the effects of resveratrol, which was also found to reduce cardiovascular and liver pathologies in conjunction with increased survival¹⁹.

Whole-body fat mass (Fig. 2b), assessed by nuclear magnetic resonance (NMR) spectroscopy and presented as the average of measurements collected longitudinally at 64, 80 and 94 weeks of age, doubled in the HFD mice compared with SD and this increase was significantly reduced by treatment with the high dose of SRT1720. Serum high density lipoprotein (HDL), positively associated with cardiovascular health, was increased in HFD-H above all other diet groups, including SD (Fig. 2b). This effect occurred despite an equivalent increase in total cholesterol in all high-fat

diets (Supplementary Fig. 3c). Because our current observations of improved body composition and structural changes in liver and pancreas with SRT1720 treatment suggest more efficient regulation of glucose homeostasis, we quantified serum levels of glucose and insulin in fasting mice (Fig. 2b). While circulating glucose was unchanged by the high-fat diet, insulin levels were more than doubled in the HFD compared with SD and HFD-H. In a similar fashion elevation of the homeostasis model assessment (HOMA) value (which evaluates insulin resistance) was blocked by treatment with SRT1720 which is consistent with the observation that SRT1720 enhanced insulin sensitivity in mice infused with glucose under a hyperinsulinemic-euglycemic clamp¹².

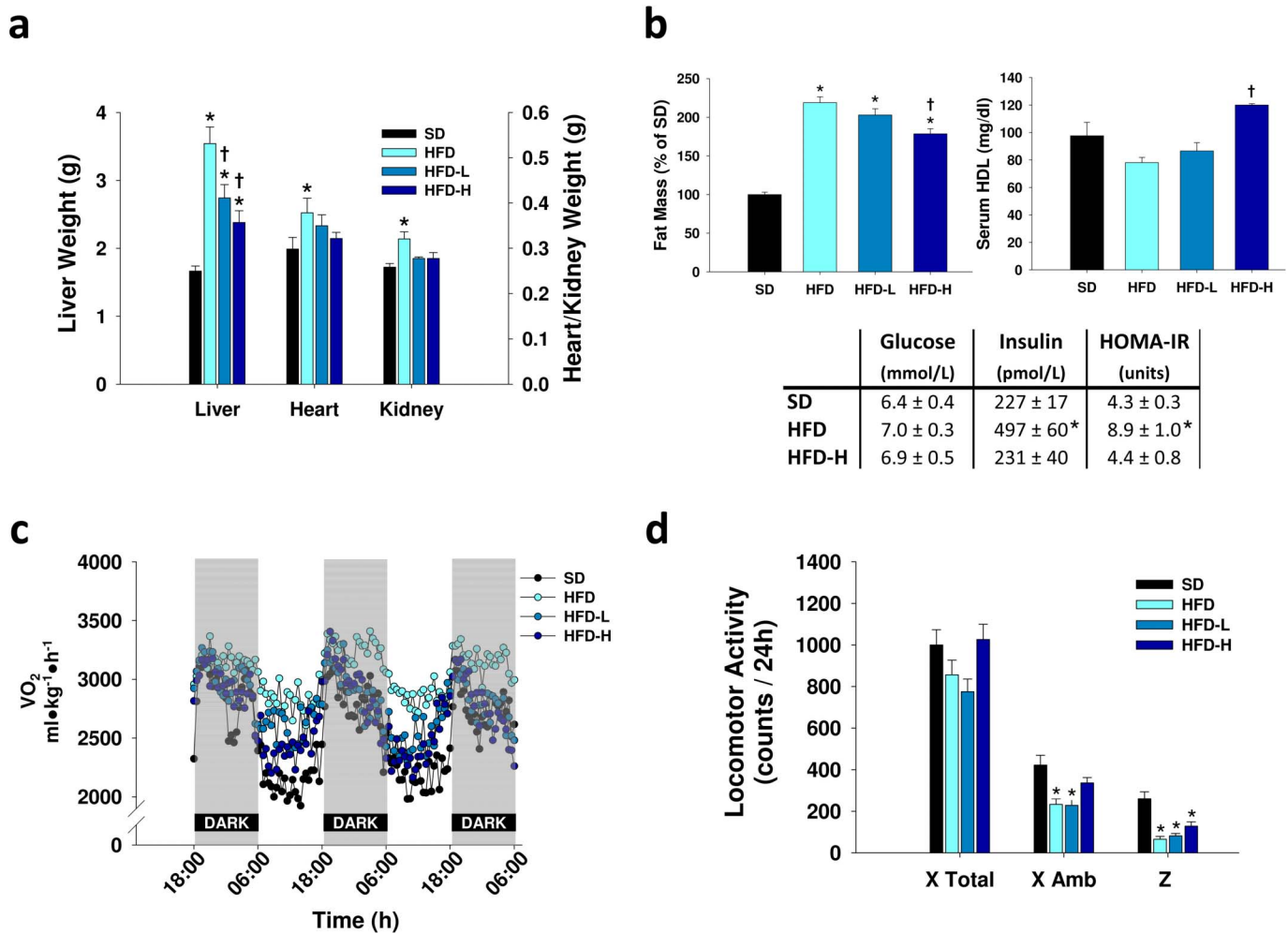


Figure 2 | SRT1720 mitigates the negative physiological implications of a high-fat diet in mice. (a) Organ weights were significantly increased in the HFD mice compared with SD and reduced by SRT1720 ($n = 6$; age = 82 wks; diet = 26 wks). (b) Fat mass increased in all high fat groups relative to SD, however fat mass was significantly reduced in HFD-H compared with HFD ($n = 15$ at 64, 80 and 94 weeks of age). HDL cholesterol was increased in sera from HFD-H mice ($n = 6$; age = 82 wks; diet = 26 wks). While serum glucose was unchanged, serum insulin was increased in HFD but not in HFD-H compared with SD. The HOMA calculation of insulin resistance was likewise increased in the HFD but not the SRT1720-treated group ($n = 8$; age = 40 weeks; diet = 12 weeks). (c) Circadian rhythm of oxygen intake over 60 h is plotted without error bars for clarity (see Supplementary Fig. 4a for average VO₂ during light and dark cycles with SEM) ($n = 14$ (SD), 12 (HFD), 10 (HFD-L), 14 (HFD-H); age = 122 wks; diet = 66 wks). (d) Daily locomotor activity represented as total movement along the horizontal plane (X Total), ambulatory movement along the horizontal plane (X Amb) and movement across the vertical axis (Z). Ambulatory and vertical movement was reduced in the HFD groups compared with SD, and the high dose of SRT1720 reversed this effect in ambulatory movement ($n = 14$ (SD), 12 (HFD), 10 (HFD-L), 14 (HFD-H); age = 122 wks; diet = 66 wks). Data are represented as the mean ± SEM. * $P < 0.0083$ from SD; † $P < 0.0083$ from HFD.

To further investigate the underlying effects involved in the observed changes to lifespan and body composition we assessed the metabolic and locomotor effects of SRT1720 in the mice at 122 weeks of age (Fig. 2c and 2d). The VO₂ for all mice displayed the expected diurnal rhythm of increased VO₂ during the dark period (when mice are normally more active and feeding). The HFD mice, however, had an increased VO₂ compared with SD controls, which was most apparent during the light cycle (Supplementary Fig. 4a). Interestingly, SRT1720 reversed this trend in the HFD-L and HFD-H groups. There was no change to VCO₂ production or the respiratory exchange ratio related to diet treatment (Supplementary Fig. 4b and 4c). Regarding locomotion, while there was no difference in total X-axis activity (which includes grooming and feeding movements performed in a stationary position), the HFD and HFD-L mice were less ambulatory along the X axis than SD controls. All HFD groups were less active vertically (on the Y axis) than SD controls. These results were similar to those obtained using another test of locomotor activity, the inclined screen test, wherein the HFD mice covered a

significantly shorter distance than the SD controls but the HFD-H mice did not (Supplementary Fig. 4c).

SRT1720 suppresses hepatic apoptosis and normalizes gene expression in obese mice. To more clearly determine the molecular basis for the preservation of health and survival by SRT1720 in animals consuming a high-fat diet, we next examined its effects on apoptotic markers and transcription in the liver. We found that SRT1720 treatment blocked an increase in markers of apoptosis, namely caspase 3 activity and DNA fragmentation, incurred by the HFD relative to SD controls (Fig. 3a). Apoptotic cell death in the hearts was likewise prevented by the drug treatment (Supplementary Fig. 3d), corroborating observations of reduced apoptosis and cleaved caspase 3 expression in mouse kidneys with ureteral obstruction treated with SRT1720¹⁸. Assessment of global changes in gene expression was performed using whole-genome microarray followed by parametric analysis of geneset enrichment (PAGE) on the livers. Similar to the effects of resveratrol^{7,21–24}, SRT1720 induced a

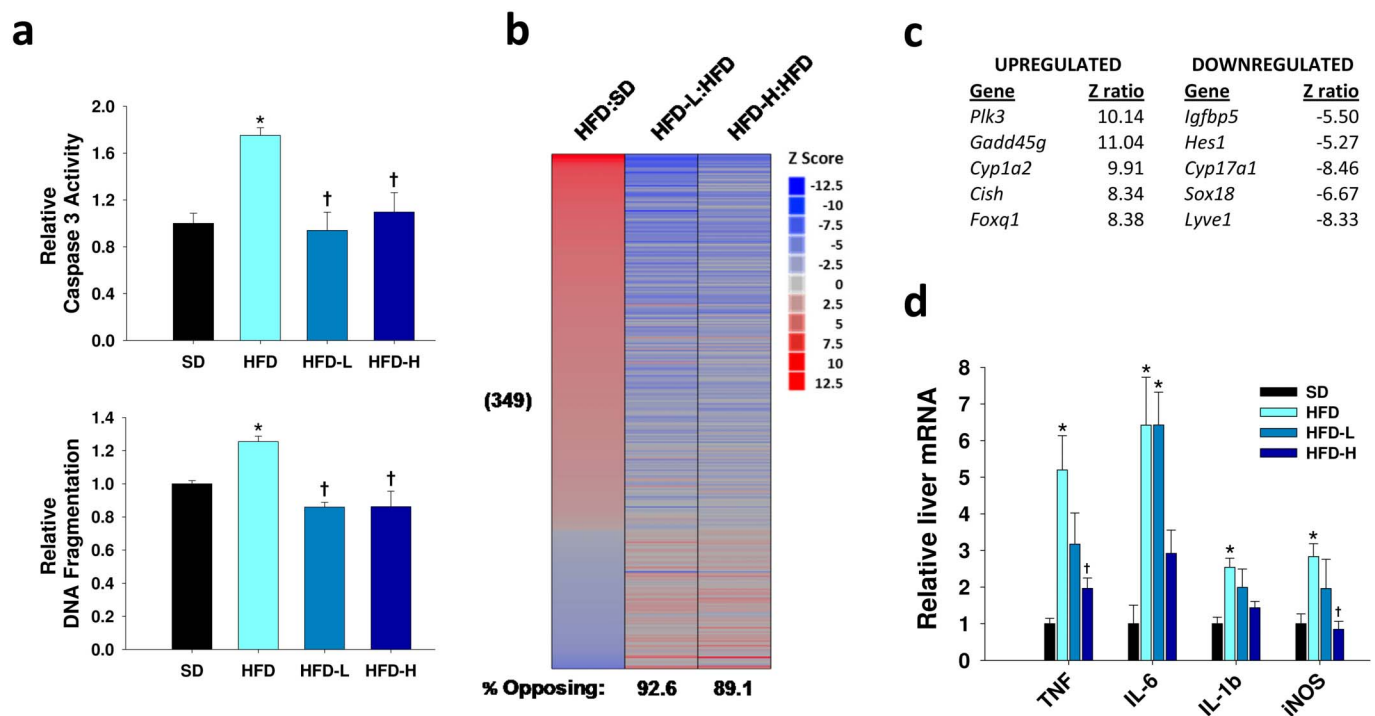


Figure 3 | SRT1720 suppresses apoptosis and restores a more normal gene expression profile indicative of reduced inflammation in the livers of mice fed a high-fat diet. (a) Two indicators of increased programmed cell death, caspase 3 activity and DNA fragmentation, were increased in the HFD compared with SD. This effect was completely blocked by both doses of SRT1720 ($n = 6$; age = 82 wks; diet = 26 wks). (b) Parametric analysis of gene-set enrichment (PAGE) comparing every pathway significantly upregulated (red) or downregulated (blue) by HFD (as compared with SD, 349 pathways of 1687 considered), and the corresponding effects of the low and high doses of SRT1720 on those same pathways ($n = 3$; age = 82 wks; diet = 26 wks). (c) The five most highly upregulated and downregulated named genes, based on fold-change in HFD-R compared to HFD (filtering on a false discovery rate of <0.05). (d) Multiple pro-inflammatory markers including TNF, IL-6, IL-1 β and iNOS were increased in the HFD mice relative to SD. No significant increase from SD was seen in the HFD-H group, and there was a significant decrease from HFD in the TNF and iNOS expression of the HFD-H livers ($n = 6$; age = 82 wks; diet = 26 wks). * $P < 0.0083$ from SD; † $P < 0.0083$ from HFD.

profound shift away from expression patterns induced by a high-fat diet. Of the pathways that were significantly changed by the high-fat diet, the low and high doses of SRT1720 induced opposing effects in 92.6% and 89.1% of cases, respectively (Fig. 3b). In particular, SRT1720 treatment suppressed genes in the liver that have previously been shown to correlate with aging in studies on kidney and brain, and decreased expression of several gene sets associated with inflammatory changes (Supplementary Table 4a). A subset of expression changes was verified by polymerase chain reaction with reverse transcription (RT-qPCR) (Supplementary Table 4b,c).

The most highly affected transcripts are presented in Figure 3c, and the complete data set is available at <http://www.ncbi.nlm.nih.gov/geo>, accession number GSE19102. Intriguingly, this short list includes *Hes1*, a known interacting partner of Sirt1²⁵, as well as *Gadd45*, a DNA repair factor that has been shown to be regulated via Sirt1-dependent deacetylation of FOXO transcription factors²⁶. It also includes *Plk3*, which is at least partially under the control of NF κ B, and might have been expected to decrease, rather than increase, due to the inhibitory effect of Sirt1 on NF κ B transactivation. We therefore attempted to ask whether our transcriptional data more broadly support the activation of Sirt1 by SRT1720. Unfortunately, this is a very difficult question to address at present, since microarray results are not available from mice overexpressing Sirt1, and post-translational modifications induced by Sirt1 are far better characterized than are the resulting transcriptional consequences.

A small set of transcriptional changes suggestive of increased gluconeogenesis and adiponectin signaling, decreased inflammation, and alterations in antioxidant defenses and lipid metabolism have been identified in the livers of mice with enhanced SIRT1 activity (two BAC-transgenic strains^{8,9}) and another strain lacking the Sirt1

inhibitory protein DBC1²⁷. Of these 12 genes, 9 were represented on our arrays, and 4 were changed to a statistically significant degree ($P < 0.05$), 3 in the predicted direction and one in the opposite, albeit with relatively small absolute effects (Supplementary Table 4d). Therefore, these results are not conclusive, but do provide suggestive evidence for an increase in gluconeogenesis (increased expression of glucose-6-phosphatase and IGFBP1) and adiponectin signaling (upregulation of adiponectin receptor 2) following treatment with SRT1720. The most likely reason we did not detect a more compelling overlap with prior studies is because our mice were sacrificed in the fed state, when gluconeogenesis is normally suppressed, whereas prior studies were performed in fasted animals or in isolated, stimulated hepatocytes. Because neither of the inflammatory markers that were suppressed by SIRT1, tumor necrosis factor (TNF) and interleukin-6 (IL-6), passed the quality control analysis on our arrays, we assayed these transcripts by RT-PCR. We found a dose-dependent suppression of both genes by SRT1720 (Fig. 3d), indicating that this compound and SIRT1 have similar anti-inflammatory effects.

Because we noted a number of transcriptional changes in the PAGE analysis that might be considered pro-inflammatory (for example, a small increase in NF κ B-related genes), we also sought to directly test the effect of SRT1720 on additional markers of inflammation in the high fat groups. We found that expression of interleukin 1 β (IL-1 β), and inducible nitric oxide synthase (iNOS), like TNF and IL-6, were elevated by the HFD relative to SD, and that both doses of SRT1720 tended to suppress these inflammatory changes in both liver and heart, although the effects were not significant in all cases (Fig. 3d and Supplementary Fig. 3e). Circulating levels of IL-6 in the serum of the HFD mice were also reduced by SRT1720 (Supplementary Table 4e). In support of the conclusion



that SIRT1720 reduces inflammation, accumulation of isoprostanes (indicative of lipid peroxidation and oxidative stress) was increased by the high-fat diet but kept at SD levels by both doses of the drug (Supplementary Fig. 3f).

Since both resveratrol and SIRT1720 have been proposed to work through a common target—Sirt1—we tested whether the transcriptional signatures induced by these two treatments showed overlapping effects. Indeed, we observed a statistically significant correlation between the effects of resveratrol and SIRT1720 (Supplementary Fig. 5). Specific transcripts that are regulated in common have been tabulated in Supplementary Table 4f. These include a number of genes that encode cytochrome P-450 enzymes, which are known to be altered in long-lived dwarf mice as well as by calorie restriction²⁸. Additionally, SIRT1720 decreased expression of complement component 1q, which has emerged as a robust expression biomarker of aging that, in cerebellum, is both increased with age and suppressed by calorie restriction²².

PGC-1 α hepatic acetylation levels are preserved and mitochondrial biogenesis is increased by SIRT1720. To confirm the activation of Sirt1 by SIRT1720 *in vivo* we analyzed the acetylation levels of PGC-1 α , a direct target of Sirt1, in the liver of 40 week old mice treated on diets for 12 weeks. The HFD group showed a dramatic increase in PGC-1 α acetylation in the liver compared with SD controls (Fig. 4a). Induction of PGC-1 α acetylation by high-fat intake has been reported in muscle²⁹. Treatment with SIRT1720 attenuated this effect (Fig. 4a), which is consistent with a previous report where SIRT1720 decreased relative PGC-1 α acetylation¹². In contrast to the liver, PGC-1 α acetylation was not reduced by SIRT1720 treatment in the muscle (Supplementary Fig. 6a). We further found that SIRT1720 promoted the deacetylation of two different Sirt1 substrates, p53 and histone H4, at low micromolar concentrations *in vitro* (Supplementary Fig. 6b,c).

To more closely assess the role of Sirt1 in mediating SIRT1720's effects *in vitro* we employed mouse embryonic fibroblasts (MEFs) that were derived from either SIRT1 knockout (KO) or wild type mice (WT). Given that previously we have shown that Sirt1 activation improves mitochondrial function^{7,30}, in the current study we assessed the ability of SIRT1720 to increase the capacity for mitochondrial respiration in the MEFs. Oxygen consumption during carbonyl cyanide 4-(trifluoromethoxy)phenylhydrazone (FCCP)-uncoupled respiration was compared with basal respiration with or without treatment with 1 μ M SIRT1720. SIRT1720-treated WT MEFs showed a significant increase in their capacity for O₂ intake while KO MEFs did not, suggesting Sirt1 is required for SIRT1720-driven increases to mitochondrial biogenesis (Fig. 4b). The current results agree with previous reports in which both Sirt1 overexpression and resveratrol treatment have been shown to increase mitochondrial biogenesis^{7,30,31}, and a recent report showing increased mitochondrial biogenesis in cultured renal proximal tubular cells treated with SIRT1720³². While these data indicate the SIRT1720-treated WT MEFs had an increased capacity for respiration, this does not necessarily translate to increased basal metabolism, as both the MEFs (Supplementary Fig. 6d) and the mice (Fig. 2c) exhibited normal or decreased O₂ intake under basal conditions. This agrees with data collected under calorie restriction, which either lowers³³ or does not affect skeletal muscle mitochondrial oxygen consumption³⁴. These observations hint at the possibility that Sirt1 activation by calorie restriction or resveratrol may induce the proliferation of mitochondria with efficient electron transport systems resulting in lower whole-body oxygen consumption.

We also assessed the Sirt1-dependence of increased stress resistance by SIRT1720 (Fig. 4c). WT MEFs that were primed by incubation with SIRT1720 at 1 or 3 μ M showed increased survival compared with untreated controls when treated with 500 μ M H₂O₂ for 24 h while MEFs from KO mice, in contrast, did not. This Sirt1

dependence may relate to Sirt1's action on p53, as we also observed increased deacetylation of p53 in the WT MEFs as compared to the KO MEFs (Supplementary Fig. 6e).

To better understand the involvement of PGC-1 α in SIRT1720's effects on cellular metabolism we employed HepG2 cells transfected with siRNA that was either non-targeting or was specific for PGC-1 α 1 and 2 (Supplementary Figure 7). SIRT1720 treatment resulted in increased mitochondrial membrane potential (Fig. 4d) and cellular ATP content (Fig. 4e) in non-targeting siRNA transfected cells and this effect was blocked by PGC-1 α knockdown.

Mitochondrial respiratory capacity is not affected by SIRT1720 in Sirt1 knockout mice. To further explore the Sirt1-dependency of SIRT1720's effects on respiration we generated a conditional Sirt1 knockout mouse to measure oxygen consumption in mitochondria isolated from the liver. Oxygen consumption during state 3 respiration was suppressed by HFD and maintained by SIRT1720 treatment in wild type mice but not in the Sirt1 knockouts (Fig. 5a). State 4 respiration was not affected by Sirt1 knockout, HFD or SIRT1720 treatment (Fig. 5b). Both the respiratory control ratio (RCR; state 3/state 4) (Fig. 5c) and FCCP-induced respiration (Fig. 5d) were reduced by HFD and oxidative capacity was only rescued by SIRT1720 treatment in mitochondria from wild type mice and not in knockout mice, demonstrating that the ability of SIRT1720 to increase respiration is Sirt1-dependent *in vitro* and *in vivo*.

Discussion

The current study shows that SIRT1720, a member of a class of drugs that are *in vitro* Sirt1-activators, has a number of long-term benefits in mice that include shifting physiological parameters in mice consuming a high-fat diet towards those consuming a standard diet, modulating gene expression pathways associated with longevity, and improving overall health. These effects led to improvements in a variety of measures including survival, motor function, insulin sensitivity, organ pathology, and metabolic activity. With regards to energy metabolism, SIRT1720 improved insulin sensitivity, maintained liver and pancreatic function, and prevented several metabolic changes associated with a high-fat diet. At the molecular level, SIRT1720 reversed the gene expression profile induced by the high-fat diet with regards to markers of inflammation, apoptosis and oxidative stress. *In vivo*, SIRT1720 promoted the deacetylation of hepatic PGC-1 α , a known Sirt1 target that regulates mitochondrial biogenesis, stress resistance and survival³⁵. *In vitro*, SIRT1720-driven increases in cell survival and mitochondrial respiration were also Sirt1-dependent. While both mean and maximum lifespans were significantly extended in the mice, mean lifespan extension through reduction of premature death and increased healthspan was the most overt benefit of SIRT1720 treatment. This is in agreement with a recent report where transgenic mice overexpressing Sirt1 displayed increased glucose tolerance and reduced susceptibility to induced tumors but not increased survival when fed a standard diet³⁶. In the case of our mice, which were subjected to metabolic stress by the high fat diet, SIRT1720 was able to dramatically shift the lifespan curves towards a more rectangular shape by acting to prevent premature death.

Our results continue to support the beneficial pharmacological effect of SIRT1720 in models of metabolic disease despite a recent report by Pacholec and colleagues to the contrary¹⁴ where the authors report 100 mg/kg SIRT1720 is not tolerable and increases mortality in mice and that the compound does not elicit beneficial effects in the *Lep^{ob/ob}* mouse model of diabetes. This conclusion is inconsistent with not only our findings but also several additional studies where SIRT1720 has been reported to exert positive effects in multiple models of metabolic disease including *Lep^{ob/ob}* mice¹¹, diet-induced obese mice^{11,12}, MSG-induced hypothalamic obese mice¹⁵ and Zucker *fa/fa* rats^{11,13}. Pacholec and colleagues did report that fasting insulin levels

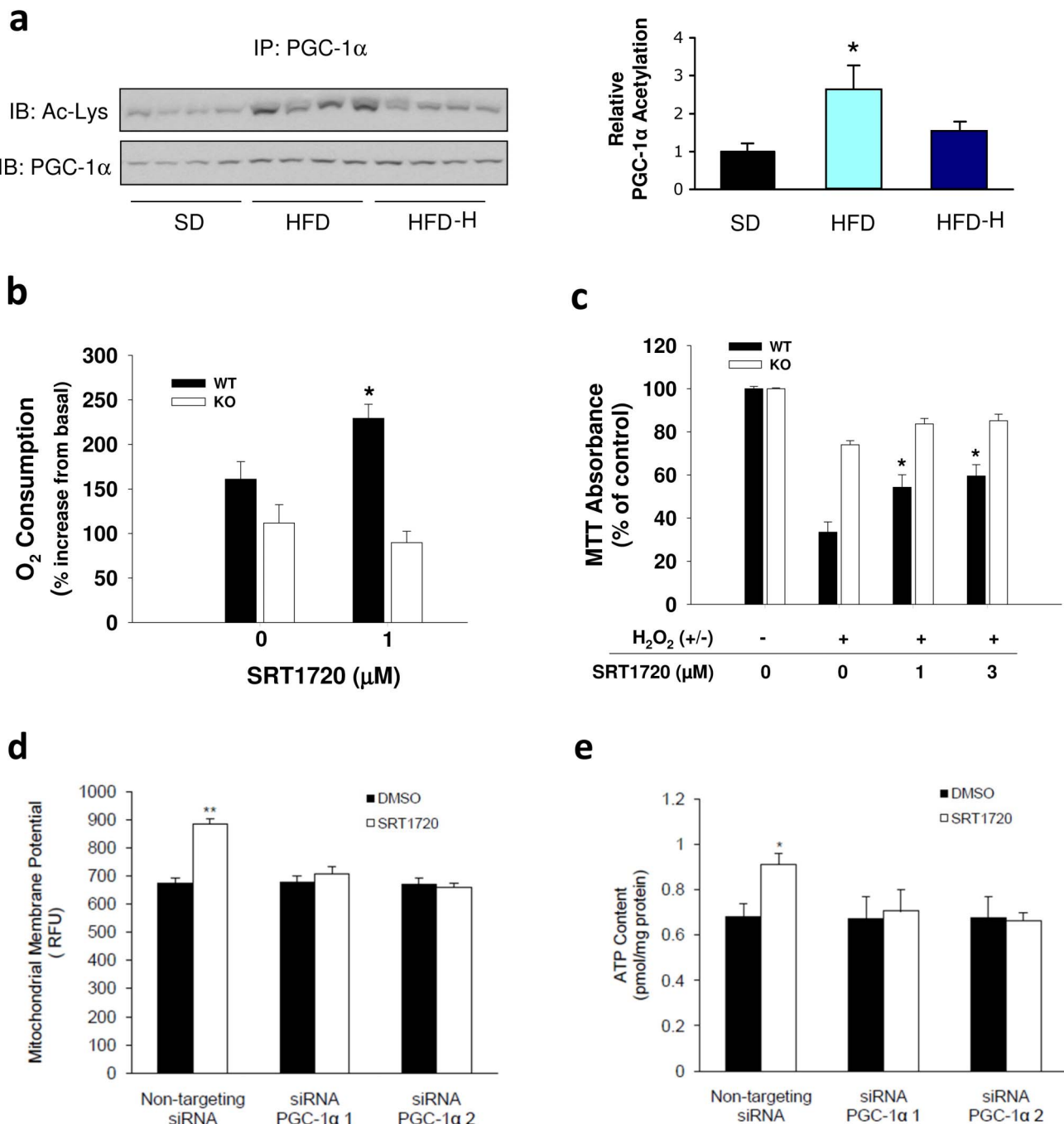


Figure 4 | SIRT1720 reduces PGC-1 α acetylation in the liver *in vivo* and increases cell survival and respiration *in vitro*. (a) Relative PGC-1 α acetylation was analyzed by immunoprecipitation from nuclear extracts from the liver followed by an immunoblot against acetylated lysine residues ($n = 8$; age = 40 weeks; diet = 12 weeks). Data are represented as the mean \pm SEM. $*P < 0.0083$ from SD. (b) Oxygen consumption in stimulated, respiration-uncoupled MEFs is expressed as the percent increase over basal respiration. Compared with vehicle-treated cells, only WT MEFs displayed increased capacity for O₂ consumption. $*P < 0.05$ from 0 μ M. (c) Cell survival following oxidative stress by 24 h exposure to H₂O₂ (500 μ M) showed increased survival after pretreatment with SIRT1720 was confined to the WT MEFs. (d) Increases to mitochondrial membrane potential in HepG2 cells only occurred in cells that were transfected with non-targeting siRNA, and this effect was blocked by siRNAs that targeted PGC-1 α 1 and 2. (e) Concurrently an increase in cellular ATP content was dependent on PGC-1 α . Data are represented as the mean \pm SEM. $*P < 0.0083$ from 0 μ M.

are reduced by SIRT1720 administration¹⁴, which is in agreement with our findings (Fig. 2) and with data reported previously in diet-induced obese mice¹¹. The putative toxicity of SIRT1720 administered at a 100 mg/kg oral dose to 8 mice over 18 days¹⁴ is inconsistent with a study where the compound exhibited no toxicity at a 5-fold higher dose for 15 weeks¹² nor is it consistent with our long-term feeding study involving over 100 mice consuming an

equivalent daily dose. In fact, our mice showed increased survival and improvement in multiple physiological parameters in response to SIRT1720 treatment and did not display overt signs of toxicity even after more than 80 weeks of treatment.

There is also ongoing debate as to whether SIRT1720 and resveratrol are direct activators of Sirt1^{11,14,15,37–39}. The data cited in argument against direct activation by these compounds are derived from

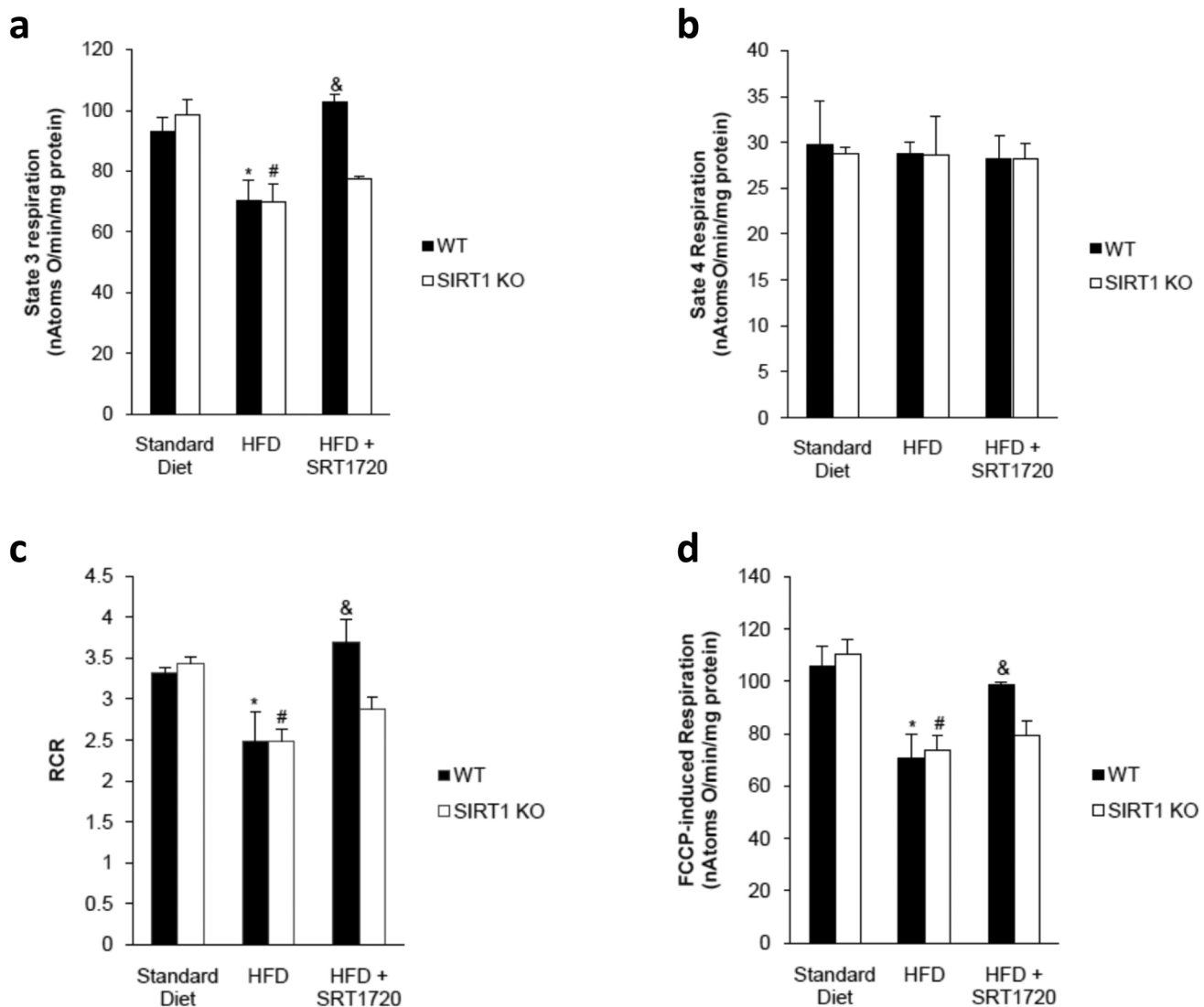


Figure 5 | SIRT1720 rescues respiratory capacity in mitochondria from wild type mice treated with a high fat diet but not after Sirt1 knockout. (a) State 3 oxygen consumption by mitochondria isolated from the liver was reduced by HFD. Treatment with SIRT1720 in the HFD was protective only in WT mice. (b) Oxygen consumption during state 4 respiration was unchanged by diet or genetic manipulation. (c) The respiratory control ratio was also reduced by HFD and rescued by SIRT1720 only in WT mice, as was FCCP-induced respiration (d). $n = 4$ mice per group; age = 30–32 weeks; diet = 18 weeks. Data are represented as the mean \pm SEM. * $P < 0.05$ from WT SD, # $P < 0.05$ from KO SD, & $P < 0.05$ from WT HFD.

biochemical assays that are poorly understood in terms of how well they model the cellular and *in vivo* settings in which beneficial effects have been demonstrated, including those in our current study (Fig. 4, Supplementary Fig. 10,12) and in previous studies^{12,13,16,40–42}. Furthermore, SIRT1720 and resveratrol have been shown to induce parallel transcriptional changes to mouse liver gene expression both here (Supplementary Fig. 5) and elsewhere²¹. The transcriptional and physiological correlations and the Sirt1-dependence both *in vitro* and *in vivo* suggest a common mechanism. At present the simplest explanation is that the target is Sirt1, which agrees with multiple cellular assays demonstrating Sirt1-dependency reported here (Fig. 4, Supplementary Fig. 10,12) and elsewhere^{12,13,16,40–42}. It should be noted, however, that the present *in vivo* effects by SIRT1720 on healthspan or lifespan do not distinguish between direct and indirect Sirt1 activation. What our data show conclusively is that long-term treatment of obese mice with SIRT1720 allows them to live healthier, more vigorous lives and the noteworthy significance of these findings is that potent molecules may one day be developed at the bench and translated to clinical practice for the promotion of healthspan and lifespan in humans.

Methods

Animals and diets. Male C57BL/6J mice were obtained from the Jackson Laboratory (Bar Harbor, ME) at 15 weeks of age and held at the Holabird NIA/NIH research facility in Baltimore, MD. During the initial holding period the mice were housed in groups of 4 with *ad libitum* access to a standard chow diet (2018 Teklad Global 18% Protein Rodent Diet, Harlan Teklad, Madison, WI) and tap water until 52 weeks of age at which time the mice were separated into groups of 3. Random cages with in each group were designated for different experimental procedures (e.g. NMR) from which to select mice as needed throughout the study. At 56 weeks the mice were randomized into four diet groups of 108 mice each after which the mice were fed either a standard AIN-93G diet (SD; carbohydrate:protein:fat ratio of 64:19:17 percent of kcal) or a high fat diet consisting of AIN-93G modified to provide 60% of calories from fat (HFD; carbohydrate:protein:fat ratio of 16:23:61). SIRT1720 was added to the HFD at a low dose (0.6 g/kg, HFD-L) and a high dose (2.0 g/kg, HFD-H) that were formulated to provide daily doses of approximately 30 mg/kg and 100 mg/kg, respectively, to the mice. The study diets were purchased from Dyets, Inc. (Bethlehem, PA) and SIRT1720 was provided by Sirtris Pharmaceuticals, Inc. (Cambridge, MA). Throughout the duration of the study all groups had *ad libitum* access to weighed amounts of their prescribed diet and water with body weight and food intake monitored twice monthly.

Because the Holabird facility was discontinued for use by the NIA in October of 2008, the mice were moved to the Gerontology Research Center of the NIA, also in Baltimore, MD, at 111 weeks of age. Both facility animal rooms were maintained at 20–22°C with 30–70% relative humidity and a 12 hour light/dark cycle. No significant



alteration to body weight, food intake or survival was noted in the two weeks after the move. All animal protocols were approved by the Gerontology Research Center Animal Care and Use Committee (352-LEG-2009) of the National Institute on Aging and by the Harvard Medical School Standard Committee on Animals.

Survival study. Animals were inspected daily for health issues and deaths were recorded for each animal. Moribund animals were euthanized by CO₂ asphyxiation and recorded. Every animal found dead or euthanized was necropsied. Criteria for euthanasia were based on an independent assessment by a veterinarian according to AAALAC guidelines and only cases where the condition of the animal was considered incompatible with continued survival are represented as deaths in the curves. Animals removed at sacrifice were considered as censored deaths.

Histology. The mice were fasted overnight. Following euthanasia, organs were excised and either frozen in liquid nitrogen or fixed in 4% paraformaldehyde. Oil red O staining on frozen liver was performed by Histoserv Inc. (Germantown, MD) and fixed tissues were stained with hematoxylin and eosin and then scored blindly for overall pathology.

Serum markers and HOMA calculation. Plasma concentrations of ALT, AST, HDL and total cholesterol were measured using the Cobas Integra 400 automated analyzer (Roche Diagnostics, Basel, Switzerland). Glucose was measured in whole blood using the Ascensia Elite glucose meter (Bayer, Mishawaka, IN). For insulin measurements, whole blood was allowed to clot for 30 min and spun at 14,000 rpm in a benchtop centrifuge for 7 min to pellet blood cells after which the serum was transferred to a fresh tube and stored at -80°C . The hormones were then measured by enzyme-linked immunosorbent assay (ELISA, Crystal Chem Inc., Downers Grove, IL) according to the kit manufacturers' instructions. Insulin resistance was calculated from fasted glucose and insulin values using the HOMA2 Calculator software available from the Oxford Centre for Diabetes, Endocrinology and Metabolism, Diabetes Trials Unit website (www.dtu.ox.ac.uk).

Pancreatic islet immunofluorescence and quantification. Mouse pancreata were fixed in 4% paraformaldehyde, embedded in OCT compound (Tissue-Tek; Electron Microscopy Sciences, Hatfield, PA), frozen, and stored at -80°C . Tissues were then cut with a cryostat to yield sections 7–10 μm thick. Antigen retrieval (Biogenex, San Ramon, CA) was used on all sections. Slides were mounted using PermaFluor (Thermo Scientific, Waltham, MA) and Nuclei were labeled with TOPRO-3 (Molecular Probes, Carlsbad, CA). Tissue was incubated with primary insulin and glucagon antibodies and secondary antibodies for pancreatic immunofluorescence from the Jackson ImmunoResearch Lab (West Grove, PA). Images were captured using a Zeiss LSM 410 confocal microscope.

Body composition. Measurements of lean, fat and fluid mass in whole, live mice were acquired by nuclear magnetic resonance (NMR) using the Minispec LF90 (Bruker Optics, Billerica, MA).

Echocardiography. Detailed methods are included in the Supplementary Information.

Metabolic and physical activity. Detailed methods are included in the Supplementary Information.

Inclined screen. Detailed methods are included in the Supplementary Information.

Quantitative real-time PCR. Detailed methods are included in the Supplementary Information.

Apoptosis and isoprostan. Detailed methods are included in the Supplementary Information.

Microarray. Detailed methods are included in the Supplementary Information.

PGC-1 α deacetylation. PGC-1 α deacetylation was evaluated by immunoprecipitating 500–1000 mg of total proteins from liver or muscle with PGC-1 α antibody, followed by immunoblotting against acetylated lysine or against PGC-1 α . All antibodies were from Cell Signaling (Cell Signaling Technology, Inc., Danvers, MA), and detection was performed using ultrasensitive horseradish peroxidase chemiluminescence (Pierce Protein Research Products, a division of Thermo Fisher Scientific Inc., Rockford, IL).

Cell culture, survival and mitochondrial biogenesis. Detailed methods are included in the Supplementary Information.

Oxygen consumption. Oxygen consumption in Sirt1 WT and KO MEFs was measured using the Seahorse 24XF instrument (Seahorse Biosciences, North Billerica, MA) according to company protocols. Cells were seeded into a seahorse tissue culture plate at a density of 40,000 cells per well and 16 h after seeding either 0.025% DMSO or 1 μM SRT1720 was added to the wells. 24 h later media was changed to unbuffered XF assay media at pH 7.4 (Seahorse Biosciences, North Billerica, MA) supplemented with 25 mM glucose (Sigma-Aldrich, St. Louis, MO) and 1 mM sodium-pyruvate and 1 mM glutamax (Invitrogen, Carlsbad, CA). Cells were incubated for 1 h at 37°C at ambient O₂ and CO₂ concentration before measurements

were taken. Respiration was measured in 4 blocks of 3 times 3 minutes. The first block measured the basal respiration rate. Next 1 μM oligomycin (EMD chemicals, Gibbstown, NJ) was added to inhibit complex V and the second block was measured. Then 0.3 μM carbonyl cyanide 4-(trifluoromethoxy)phenylhydrazone (FCCP) (Sigma-Aldrich, St. Louis, MO) was added to uncouple respiration and the third block was measured. Finally 2 μM antimycin A (Sigma-Aldrich, St. Louis, MO) was added to inhibit complex 3 and the last measurements were performed. Immediately after finishing the measurements cells were counted using a Beckman Z1 Coulter counter (Beckman Coulter Inc., Brea, CA).

In vitro Sirt1 deacetylase activity. Detailed methods are included in the Supplementary Information.

Western blotting and p53 deacetylation. Detailed methods are included in the Supplementary Information.

Mitochondrial function in HepG2 cells. The hepatoma-derived HepG2 cell line (ATCC) was cultured in low glucose Dulbecco's modified eagle medium (DMEM) supplemented with 10% FBS and antibiotics (Invitrogen). Cells were maintained at 37°C in 5% CO₂. For PGC-1 α knockdown experiments, cells were transfected with 30 nM siRNA or a non-targeting siRNA (Invitrogen) using Lipofectamin 2000 (Invitrogen). Cells were treated with vehicle (0.001% DMSO) or SRT1720 (final concentration of 1 μM in 0.001% DMSO) for 24 h. Mitochondrial membrane potential was measured using tetramethylrhodamine methyl ester (TMRM) (Sigma) as previously described⁴³. ATP content was measured using a commercial available kit according to manufacturer's instructions (Roche).

Sirt1 knockout experiments. Sirt1 was knocked out in adult animals using a tamoxifen-inducible whole-body Cre-loxP system based on the floxed Exon4 SIRT1 knockout mouse⁴⁴. Knockout in liver in this model is >85% based on Western blotting for Sirt1. At 12–14 weeks of age mice were placed on either HFD or HFD + SRT1720 (2g/kg in food) for 18 weeks. Mitochondria were isolated from the liver of male mice by conventional methods⁴⁵ with slight modifications⁴⁶. Protein content was determined by the biuret method⁴⁷ calibrated with bovine serum albumin. Oxygen consumption of mitochondria isolated from liver was polarographically determined with a Clark type polarographic oxygen⁴⁸ with a PC-operated electrode control unit (Oxygraph, Hansatech Instruments Ltd.). Mitochondria (1 mg) were suspended under constant stirring at 25°C , in 1.4 ml of standard respiratory medium (130 mM sucrose, 50 mM KCl, 5 mM MgCl₂, 5 mM KH₂PO₄, 50 μM EDTA, and 5 mM HEPES (pH 7.4) and 3 μM rotenone) and energized by adding succinate to a final concentration of 5 mM. State 3 respiration was induced by adding 200 nmol adenosine diphosphate (ADP). Oxygen consumption was also measured in the presence of 1 μM carbonylcyanide-*p*-trifluoromethoxyphenylhydrazone (FCCP).

Statistics. Data are expressed as means \pm standard error of the mean (SEM). Single-factor analyses of variance followed by Bonferroni-Dunn post-hoc tests were used for all comparisons. Mortality during the survival study was assessed by using the logrank test to compare the Kaplan-Meier survival curves. We compared Kaplan-Meier survival estimates among the high fat diet groups with both log-rank tests and Wilcoxon tests (SAS PROC LIFETEST). Results of both tests were consistent, so we report only the P values given by the log-rank tests. The Cox proportional hazards procedure was also used (SAS PROC PHREG). Of the 108 initial HFD mice 7 were experimental, censored deaths (1 died at 71 weeks of age due to accidental drowning by pulmonary gavage during an OGTT and 6 were culled during the sacrifice at 82 weeks of age). Of the 108 initial HFD-L mice 7 mice were experimental, censored deaths (1 died at 71 weeks of age due to accidental drowning by pulmonary gavage during an OGTT and 6 were culled during the sacrifice at 82 weeks of age). Of the 108 initial HFD-H mice 7 mice were experimental, censored deaths (1 died at 71 weeks of age due to accidental drowning by pulmonary gavage during an OGTT and 6 were culled during the sacrifice at 82 weeks of age).

- Schrager, M. A. *et al.* Sarcopenic obesity and inflammation in the INCHIANTI study. *J. Appl. Physiol.* 102, 919–925 (2007).
- Cesari, M. *et al.* Sarcopenia, obesity, and inflammation—results from the Trial of Angiotensin Converting Enzyme Inhibition and Novel Cardiovascular Risk Factors study. *Am. J. Clin. Nutr.* 82, 428–434 (2005).
- Tissenbaum, H. A. & Guarente, L. Increased dosage of a sir-2 gene extends lifespan in *Caenorhabditis elegans*. *Nature* 410, 227–230 (2001).
- Howitz, K. T. *et al.* Small molecule activators of sirtuins extend *Saccharomyces cerevisiae* lifespan. *Nature* 425, 191–196 (2003).
- Lavu, S., Boss, O., Elliott, P. J. & Lambert, P. D. Sirtuins—novel therapeutic targets to treat age-associated diseases. *Nat. Rev. Drug Discov.* 7, 841–853 (2008).
- Knutson, M. D. & Leeuwenburgh, C. Resveratrol and novel potent activators of SIRT1: effects on aging and age-related diseases. *Nutr. Rev.* 66, 591–596 (2008).
- Baur, J. A. *et al.* Resveratrol improves health and survival of mice on a high-calorie diet. *Nature* 444, 337–342 (2006).
- Banks, A. S. *et al.* Sirt1 gain of function increases energy efficiency and prevents diabetes in mice. *Cell Metab.* 8, 333–341 (2008).
- Pfluger, P. T., Herranz, D., Velasco-Miguel, S., Serrano, M. & Tschöp, M. H. Sirt1 protects against high-fat diet-induced metabolic damage. *Proc. Natl. Acad. Sci. U.S.A.* 105, 9793–9798 (2008).



10. Baur, J. A. & Sinclair, D. A. Therapeutic potential of resveratrol: the in vivo evidence. *Nat. Rev. Drug Discov.* 5, 493–506 (2006).
11. Milne, J. C. *et al.* Small molecule activators of SIRT1 as therapeutics for the treatment of type 2 diabetes. *Nature* 450, 712–716 (2007).
12. Feige, J. N. *et al.* Specific SIRT1 activation mimics low energy levels and protects against diet-induced metabolic disorders by enhancing fat oxidation. *Cell Metab.* 8, 347–358 (2008).
13. Yoshizaki, T. *et al.* SIRT1 inhibits inflammatory pathways in macrophages and modulates insulin sensitivity. *Am. J. Physiol. Endocrinol. Metab.* 298, E419–E428 (2010).
14. Pacholec, M. *et al.* SIRT1720, SIRT2183, SIRT1460, and resveratrol are not direct activators of SIRT1. *J. Biol. Chem.* 285, 8340–8351 (2010).
15. Dai, H. *et al.* SIRT1 activation by small molecules: kinetic and biophysical evidence for direct interaction of enzyme and activator. *J. Biol. Chem.* 285, 32695–32703 (2010).
16. Yamazaki, Y. *et al.* Treatment with SIRT1720, a SIRT1 Activator, Ameliorates Fatty Liver with Reduced Expression of Lipogenic Enzymes in MSG Mice. *Am. J. Physiol. Endocrinol. Metab.* 297, E1179–E1186 (2009).
17. Walker, A. K. *et al.* Conserved role of SIRT1 orthologs in fasting-dependent inhibition of the lipid/cholesterol regulator SREBP. *Genes Dev.* 24, 1403–1417 (2010).
18. Li, Y. *et al.* Hepatic overexpression of SIRT1 in mice attenuates endoplasmic reticulum stress and insulin resistance in the liver. *FASEB J.* (2011). [Epub ahead of print]
19. Pearson, K. J. *et al.* Resveratrol delays age-related deterioration and mimics transcriptional aspects of dietary restriction without extending life span. *Cell Metab.* 8, 157–168 (2008).
20. He, W. *et al.* Sirt1 activation protects the mouse renal medulla from oxidative injury. *J. Clin. Invest.* 120, 1056–1068 (2010).
21. Smith, J. J. *et al.* Small molecule activators of SIRT1 replicate signaling pathways triggered by calorie restriction in vivo. *BMC Syst. Biol.* 10, 31 (2009).
22. Park, S. K. *et al.* Gene expression profiling of aging in multiple mouse strains: identification of aging biomarkers and impact of dietary antioxidants. *Aging Cell* 8, 484–495 (2009).
23. Barger, J. L., Kaye, T., Pugh, T. D., Prolla, T. A. & Weindruch, R. Short-term consumption of a resveratrol-containing nutraceutical mixture mimics gene expression of long-term caloric restriction in mouse heart. *Exp. Gerontol.* 9, 859–866 (2008).
24. Barger, J. L. *et al.* A low dose of dietary resveratrol partially mimics caloric restriction and retards aging parameters in mice. *PLoS One* 3, e2264 (2008) [published erratum appears in: *PLoS ONE* 3 (2008)].
25. Takata, T. & Ishikawa, F. Human Sir2-related protein SIRT1 associates with the bHLH repressors HES1 and HEY2 and is involved in HES1- and HEY2-mediated transcriptional repression. *Biochem. Biophys. Res. Commun.* 301, 250–257 (2003).
26. Brunet, A. *et al.* Stress-dependent regulation of FOXO transcription factors by the SIRT1 deacetylase. *Science* 303, 2011–2015 (2004).
27. Escande, C. *et al.* Deleted in breast cancer-1 regulates SIRT1 activity and contributes to high-fat diet-induced liver steatosis in mice. *J. Clin. Invest.* 120, 545–558 (2010).
28. Swindell, W. R. Gene expression profiling of long-lived dwarf mice: longevity-associated genes and relationships with diet, gender and aging. *BMC Genomics* 3, 353 (2007).
29. Coste, A. *et al.* The genetic ablation of SRC-3 protects against obesity and improves insulin sensitivity by reducing the acetylation of PGC-1 α . *Proc. Natl. Acad. Sci. U.S.A.* 105, 17187–17192 (2008).
30. Lagouge, M. *et al.* Resveratrol improves mitochondrial function and protects against metabolic disease by activating SIRT1 and PGC-1 α . *Cell* 127, 1109–1122 (2006).
31. Wareski, P. *et al.* PGC-1 α and PGC-1 β regulate mitochondrial density in neurons. *J. Biol. Chem.* 284, 21379–21385 (2009).
32. Beeson, C. C., Beeson, G. C. & Schnellmann, R. G. A high-throughput respirometric assay for mitochondrial biogenesis and toxicity. *Anal. Biochem.* 404, 75–81 (2010).
33. López-Lluch, G. *et al.* Calorie restriction induces mitochondrial biogenesis and bioenergetic efficiency. *Proc. Natl. Acad. Sci. U.S.A.* 103, 1768–1773 (2006).
34. Lambert, A. J., Wang, B., Yardley, J., Edwards, J. & Merry, B. J. The effect of aging and caloric restriction on mitochondrial protein density and oxygen consumption. *Exp. Gerontol.* 39, 289–295 (2004).
35. Anderson, R. M. *et al.* Dynamic regulation of PGC-1 α localization and turnover implicates mitochondrial adaptation in calorie restriction and the stress response. *Aging Cell* 7, 101–111 (2008).
36. Herranz, D. *et al.* Sirt1 improves healthy ageing and protects from metabolic syndrome-associated cancer. *Nature Communications* 1, 1–8 (2010) doi:10.1038/ncomms1001.
37. Kaerberlein, M. *et al.* Substrate-specific activation of sirtuins by resveratrol. *J. Biol. Chem.* 280, 17038–17045 (2005).
38. Borra, M. T., Smith, B. C. & Denu, J. M. Mechanism of human SIRT1 activation by resveratrol. *J. Biol. Chem.* 280, 17187–17195 (2005).
39. Beher, D. *et al.* Resveratrol is not a direct activator of SIRT1 enzyme activity. *Chem. Biol. Drug Des.* 74, 619–624 (2009).
40. Liu, Y. *et al.* A fasting inducible switch modulates gluconeogenesis via activator/coactivator exchange. *Nature* 456, 269–273 (2008).
41. Yoshizaki, T. *et al.* SIRT1 exerts anti-inflammatory effects and improves insulin sensitivity in adipocytes. *Mol. Cell Biol.* 29, 1363–1374 (2009).
42. Funk, J. A., Odejinmi, S. & Schnellmann, R. G. SIRT1720 induces mitochondrial biogenesis and rescues mitochondrial function after oxidant injury in renal proximal tubule cells. *J. Pharmacol. Exp. Ther.* 333, 593–601 (2010).
43. Rolo, A. P., Palmeira, C. M. & Wallace, K. B. Mitochondrially mediated synergistic cell killing by bile acids. *Biochim. Biophys. Acta.* 1637, 127–132 (2003).
44. Cheng, H. L. *et al.* Developmental defects and p53 hyperacetylation in Sir2 homolog (SIRT1)-deficient mice. *Proc. Natl. Acad. Sci. U.S.A.* 100, 10794–10799 (2003).
45. Gazdotti, P., Malmstrom, K. & Brdiczka, D. *Membrane biochemistry: A laboratory manual on transport and bioenergetics.* In: E. Carafoli, E., Semenza, G. (Eds), Springer-Verlag, New York, pp 6–69 (1979).
46. Rolo, A. P., Oliveira, P. J., Moreno, A. J. & Palmeira, C. M. Bile acids affect liver mitochondrial bioenergetics: possible relevance for cholestasis therapy. *Toxicol. Sci.* 57, 177–185 (2000).
47. Gornall, A. G., Bardawill, C. J. & David, M. M. Determination of serum proteins by means of the biuret reaction. *J. Biol. Chem.* 177, 751–766 (1949).
48. Estabrook, R. W. Mitochondrial respiratory control and the polarographic measurements of ADP/O ratios. *Methods Enzymol.* 10, 41–47 (1967).

Acknowledgments

This research was conducted under a Cooperative Research and Development Agreement (CRADA) between Sirtris, a GSK Company, and the National Institute on Aging, National Institutes of Health (NIA/NIH). Microarray data are archived under the accession number GSE19102. JAB is supported by NIH Pathway to Independence Award R00AG031182. We are grateful to Dawn Nines, Dawn Phillips and Justine Lucas for their excellent animal care. We also thank Larry Brant for help with data analyses and Olga Carlson for technical assistance. Funding was provided by the Intramural Research Program of the NIA/NIH, the Swiss National Science Foundation and the ERC Ideas program. Funding to DAS was provided by the NIH/NIA Extramural Research Program and the Glenn Foundation for Medical Research.

Author contributions

Animal experiments were designed and carried out by R.K.M. and R.de C. Sirt1 knockout mice were generated and assayed by NP, A.G. and D.A.S. R.K.M., J.A.B. and R.de C. prepared the manuscript. K.J.P., C.H.W., J.L.E., Z.U., G.P.V., D.A.S. and P.J.E. assisted with the design and interpretation of experiments. T.M.W. assisted with the handling of animals and behavioral studies. Measures of inflammatory and apoptotic states of the livers and hearts were performed by A.C. and Z.U. B.P.H. performed the in-vitro deacetylation assays, and survival assays and protein assays were performed by E.M.M., K.A. and M.G. Immunofluorescence of pancreata were performed by Y-K.S., A.A.W. and J.M.E. Analysis of PGC-1 α acetylation was performed by C.C. and J.A. Respiration in the MEFs was assessed by M.S.-K. and V.A.B. Echocardiography was performed by M.K. and M.I.T. Microarray assays were performed by E.L. and computational methods for analysis of microarray data were developed and applied by Y.Z., W.R.S. and K.G.B. Hepatic gene expression changes related to Sirt1 were determined by P.M.I. and A.M.-M. Mitochondrial function in HepG2 cells was assayed by A.G. and hepatic mitochondrial respiration of Sirt1 knockout and wild type mice was performed by A.G. and N.P.

Additional information

Supplementary Information accompanies this paper at <http://www.nature.com/scientificreports>

Accession codes The complete microarray data set is available at <http://www.ncbi.nlm.nih.gov/geo>, accession number GSE19102.

Competing financial interests: D.A.S. consults for and J.L.E., C.H.W., G.P.V. and P.J.E. are employed by Sirtris, a GSK Company, that has a commercial interest in developing SIRT1 activators.

License: This work is licensed under a Creative Commons Attribution-NonCommercial-NoDerivative Works 3.0 Unported License. To view a copy of this license, visit <http://creativecommons.org/licenses/by-nc-nd/3.0/>

How to cite this article: Minor, R.K. *et al.* SIRT1720 improves survival and healthspan of obese mice. *Sci. Rep.* 1, 70; DOI:10.1038/srep00070 (2011).



SUBJECT AREAS:

PHARMACOLOGY

MOUSE

METABOLISM

DISEASES

SCIENTIFIC REPORTS:

1 : 70

DOI: 10.1038/srep00070
(2011)

Published:

18 August 2011

Updated:

16 January 2013

CORRIGENDUM: SRT1720 improves survival and healthspan of obese mice

Robin K. Minor, Joseph A. Baur, Ana P. Gomes, Theresa M. Ward, Anna Csiszar, Evi M. Mercken, Kotb Abdelmohsen, Yu-Kyong Shin, Carles Canto, Morten Scheibye-Knudsen, Melissa Krawczyk, Pablo M. Irueta, Alejandro Martín-Montalvo, Basil P. Hubbard, Yongqing Zhang, Elin Lehrmann, Alexa A. White, Nathan L. Price, William R. Swindell, Kevin J. Pearson, Kevin G. Becker, Vilhelm A. Bohr, Myriam Gorospe, Josephine M. Egan, Mark I. Talan, Johan Auwerx, Christoph H. Westphal, James L. Ellis, Zoltan Ungvari, George P. Vlasuk, Peter J. Elliott, David A. Sinclair & Rafael de Cabo

There are two typographical errors in Figure 2A and Figure 5B. In Figure 2A the Y axes, “Liver Weights” should read “Weights”. In Figure 5B the Y axis, “Sate 4” should read “State 4”.